

## Application of Artificial Neural Network on SHM of long-span bridges

Dinh Tung Nguyen<sup>1,\*</sup>, Xiaolin Meng<sup>1</sup>, John S Owen<sup>1</sup>, Yilin Xie<sup>1</sup>, Panagiotis Psimoulis<sup>1</sup>, George Ye<sup>2</sup>

<sup>1</sup> Faculty of Engineering, University of Nottingham, Nottingham NG7 2TU, UK

<sup>2</sup> UbiPOS UK Limited, Nottingham NG7 2TU, UK

**Key words:** *SHM; long-span bridges; regression model; Neural Network; Bayesian.*

### ABSTRACT

As key transportation infrastructure assets, long-span bridges are critical to regional cooperation and economic and social development of a country. An increase in usage and demand as well as extreme weather events are posing constant threats to these structures. An installation of Structural Health Monitoring (SHM) systems on long-span bridges are a mandatory practice in many countries to ensure their safety and serviceability. However, the diagnosis and prognosis of the reliability and damage of these structures are challenged by the sensitivity of structural performances and monitoring parameters to environmental and operational conditions. Separating effects induced by wind, temperature and traffic is therefore one of the primary objectives of the GeoSHM Demonstration Project. Funded by the European Space Agency (ESA), the aim of this project is to deliver a smart SHM data strategy to evaluate the structural health status of long-span bridges and aid bridge operators in their decision making process. Recent outcomes of this project on the one of the three tests structures – the Forth Road Bridge in Scotland, UK – will be discussed in this paper.

### I. INTRODUCTION

Long-span bridges are often among the key transportation infrastructure assets of a country, stimulating regional cooperation and economic and social development. The inevitable aging process and the accumulation of damage resulting from wind, traffic and the surrounding environment can adversely affect their performance. Without proper monitoring, maintenance and warning, the closure or collapse of these bridges is possible. This can lead to significant economic and societal impacts and, in some cases, heavy casualties as seen with the incident of the Seongsu Bridge in Seoul in 1998 (Failure Knowledge Database), the I-35W highway bridge in Minnesota in 2007 (Liao and Okazaki, 2009), the newly installed pedestrian bridge at Florida International University in Miami in 2018 (Miami Herald) or more recently, the Morandi Bridge in Genoa in 2018 (The Guardian). Therefore, Structural Health Monitoring (SHM) is vital to ensure the safety and serviceability of these structures, reducing the risk of malfunction due to extreme loading and long-term degradation.

Various SHM systems of civil engineering infrastructure have been developed significantly in recent years thanks to the evolution of sensing and communication technologies as well as data processing methodologies, including the applications of machine learning and pattern recognition. However, the very characteristics of long-span bridges have posed many challenges to the successful delivery of a SHM framework. One of the greatest obstacles is that both the response and modal frequencies of long-span bridges are highly sensitive to environmental and

operational conditions, which can mask the changes in structural characteristics caused by damages (Cross et al., 2013; Meng et al., 2018; Chen et al., 2018). Moreover, this challenge can be exacerbated by the presence of outliers in monitoring data due to technical issues and errors during data processing and storage (Dervilis et al., 2015).

Funded by the European Space Agency (ESA), the project “GNSS and Earth Observation for Structural Health Monitoring of Long-span Bridges” or GeoSHM was initiated in August 2013. Following the success of the 1.5 year Feasibility Study, this project was extended to the GeoSHM Demonstration project (ESA Website). The Forth Road Bridge (FRB) in Scotland is one of the test structures, together with two other long-span bridges in China. The aim of the GeoSHM Demonstration Project is to develop (i) an integrated sensor system featuring the use of the Global Navigation and Satellite Systems (GNSS) and the state-of-the-art Earth Observation (EO) technologies to monitor long-span bridges and (ii) an innovate GeoSHM data strategy to evaluate the structural health status of bridges and aid bridge operators in their decision making process. Separating the effects induced by wind, temperature and traffic is among the primary objectives in order to successfully deliver Point (ii).

The work presented in this paper focuses on discussing the current progress of the GeoSHM project on the FRB. The monitoring data in 2015 and 2016 will be exploited to uncover the strong dependence of the bridge response on environmental and operational conditions and the needs of separating temperature and traffic effects to facilitate further analysis. Artificial

---

\* Email address: dinh.nguyen1@nottingham.ac.uk

Neural Network (ANN)-based regression models are created to quantify these relationships and offer a means to decouple wind-induced effects from environmental and operational influences. Some outcomes of this analysis will be presented and discussed here, which lays a foundation to accomplish the ultimate objective of the GeoSHM project.

## II. STRUCTURAL HEALTH MONITORING OF THE FRB

### A. Overview of the FRB

The FRB is the major suspension bridge across the Firth of Forth, linking Edinburgh to Northern Scotland (Figure 1a). When opened in 1964, this 2.5km long bridge was the fourth longest suspension bridge in the world and the longest outside the United States of America. The 1,006m long main span of the FRB is suspended from two main cables aerially spun between two 150m high main towers; each side span is 408m long. The suspended structure is made of steel trusses and features three longitudinal air gaps, one between each footway and carriageway and one between the two carriage ways. This perforated structure gives the FRB a strong aerodynamic stability.

The main span and two side spans are connected to the main towers by pairs of truss end links, which are considered to be one of the critical elements of the FRB. In December 2015, a fracture on one of the North East truss end links connecting the main span to the North tower was detected (Figure 1b). This was followed by further inspections and an approximately one-month closure of the bridge to carry out a temporary fix. Later in February 2016, the FRB was re-open to all traffic. A plan to prevent similar failures in the future has been proposed and eventually was implemented in February 2017.

On account of the steel trusses and three longitudinal air gaps, the FRB is not prone to vortex-induced vibration or flutter but is prone to buffeting due to turbulent wind. On some occasions, such as in January 2015, strong winds caused the mid span of the FRB to move laterally by a distance of 2m away from the normal position superimposed by a 3m peak-to-peak oscillation. Such movements led to the closure of the FRB to ensure the safety of public.

### B. Description of the GeoSHM sensor system

Figure 2 describes the current status of the GeoSHM sensor system installed on the FRB. Three pairs of GNSS receivers are installed along the main span; one is at the mid span while the other two are at the navigation points. There are two other GNSS receivers located at the top of the North-East and South-West tower legs to monitor deformation of the main tower. In addition, the wind measurement is facilitated by using three WindMaster 3D sonic anemometers placed at the mid span and at the top of the two main towers. Other environmental conditions are determined by the meteorological station installed at the mid span. The

other key component of the GeoSHM sensor system is the use of the interferometric synthetic-aperture radar (InSAR) images from the Sentinel-1 satellites, which offer the remote long-term subsidence measurement of the bridge site and its surrounding areas. In the next phase, eight tri-axial Sherborne accelerometers will be installed at a number positions on the main span and main cables to complement GNSS measurements. Further accelerometers are installed on the top of the main towers together with uniaxial inclinometers to measure the inclination of the towers.

The overview of the GeoSHM system architecture is summarised in Figure 3. Data of the GeoSHM sensor system is collected at predefined sampling frequencies and transferred to the main GeoSHM servers located at University of Nottingham for processing and storage. 10-minute average statistics and modal frequencies are calculated and analysed; they are featured in real-time monitoring and, more importantly, to evaluate the structural health status (Meng et al., 2019). In the next section, some of the selected monitoring parameters will be introduced and further analysed to reveal some features of the baseline performance of the FRB including the strong influence of temperature and traffic.

### C. Influence of temperature and traffic on the performance of the FRB

Effects of temperature and traffic on the FRB are analysed by investigating the 10-minute mean and standard deviation of the bridge response measured at the mid span as well as natural frequencies of the first lateral and heaving modes. Here, the lateral (along the  $y$ -axis) and heaving (along the  $z$ -axis) responses are considered. A two week period of normal operation of the FRB (from 01 to 15/08/2018) is shown in Figure 4 and Figure 5 as an example. It is clear that effects of temperature and traffic are more visible on the heaving response of the mid span compared to the lateral response. A diurnal pattern can be observed where the 10-min standard deviation of the heaving responses during the daytime is higher than that during the night-time (Figure 5b). An increase in traffic occurs around 06:00 and leads to large dynamic responses; after 15:00, less traffic is on the FRB, causing a gradual drop of dynamic responses. This traffic-induced pattern can also be seen on the 10-minute mean of the heaving response (Figure 5a) where the sagging of the mid span is larger during the daytime due to an increase in traffic. However, natural fluctuations of the temperature make this pattern less visible. In addition, this diurnal pattern is observed on the 10-minute natural frequencies of the first lateral and heaving modes (Figure 6). During a day, an increase in the air temperature and additional mass due to traffic cause these frequencies to reduce by 7% and 2% respectively. Since there is less traffic present on the bridge at weekends, these aforementioned patterns are less pronounced.

The 10-minute mean and standard deviations of the lateral response are largely influenced by wind; therefore data appear to be more random and no clear short- and long-term trends are visible (**Error! Reference source not found.**). Using the monitoring data in 2015 and 2016, quadratic relationships between the lateral response and the normal component of the mean wind speed are clearly shown in Figure 7. Similar plots are produced for the heaving response (Figure 8**Error! Reference source not found.**); however, no clear relationship can be concluded. This is due to the strong influences of temperature and traffic as discussed earlier, which significantly masks the effects of wind on the heaving response, particularly at wind speeds below  $15\text{ms}^{-1}$ . Therefore, it is important to develop a method to remove effects of temperature and traffic to understand wind-induced responses and diagnose the structural performance of the FRB.

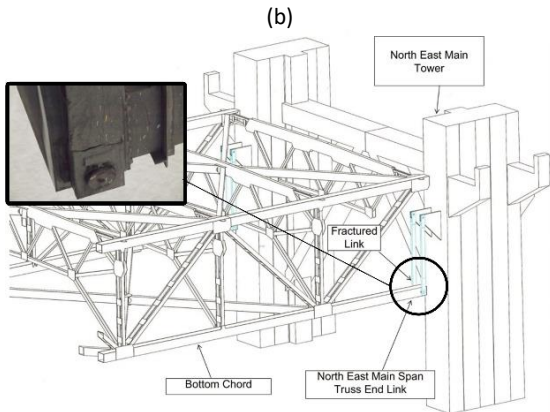
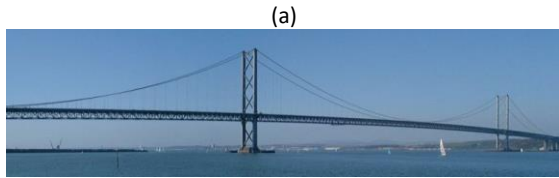


Figure 1. (a) The FRB (Scotland, UK); (b) Fractured North East truss end links ([www.newcivilengineer.com](http://www.newcivilengineer.com))

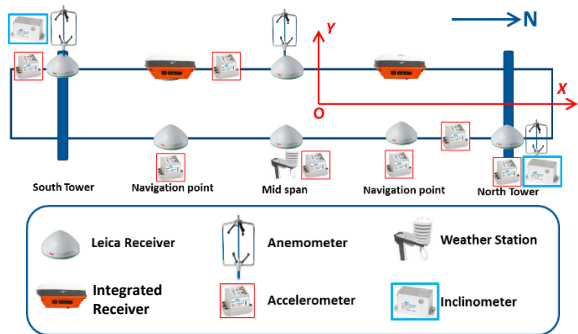


Figure 2. GeoSHM sensor system on the FRB (highlighted sensors will be installed in the next phase).

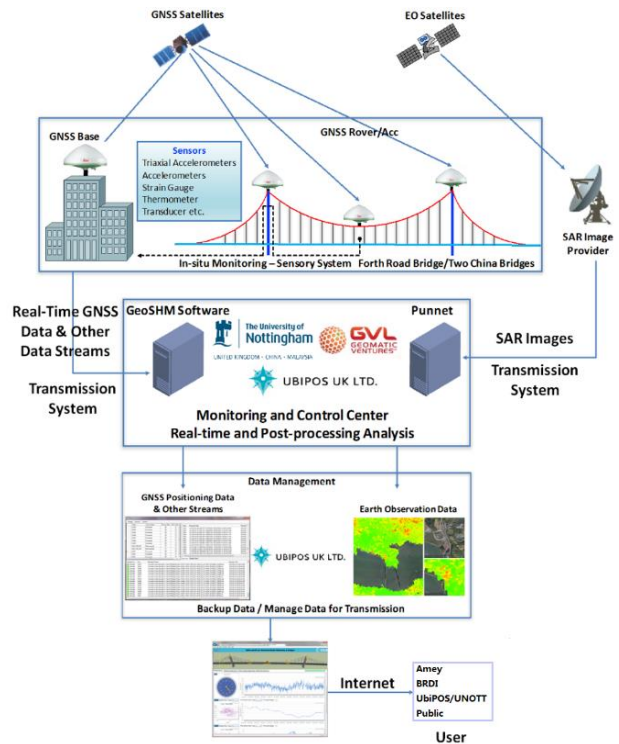


Figure 3. Overview of the GeoSHM system architecture.

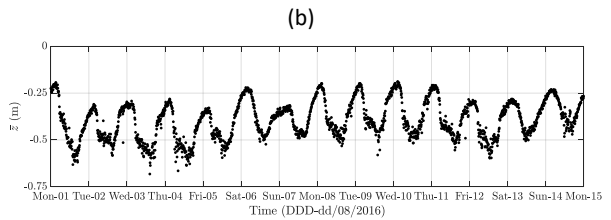
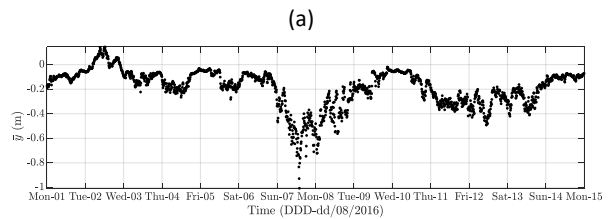


Figure 4. 10 minute (a) mean and (b) standard deviation of the lateral response (from 01 to 15/08/2016).

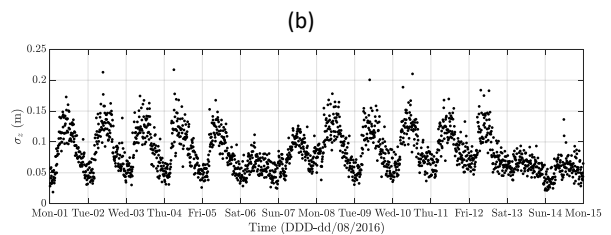
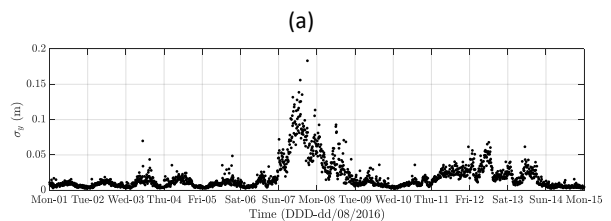


Figure 5. 10 minute (a) mean and (b) standard deviation of the lateral response (from 01 to 15/08/2018).

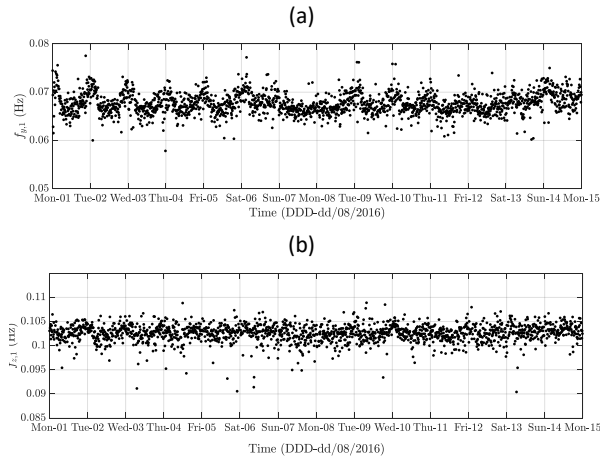


Figure 6. Estimates of 10-minute natural frequencies of the first (a) lateral and (b) heaving modes (from 01 to 15/08/2016).

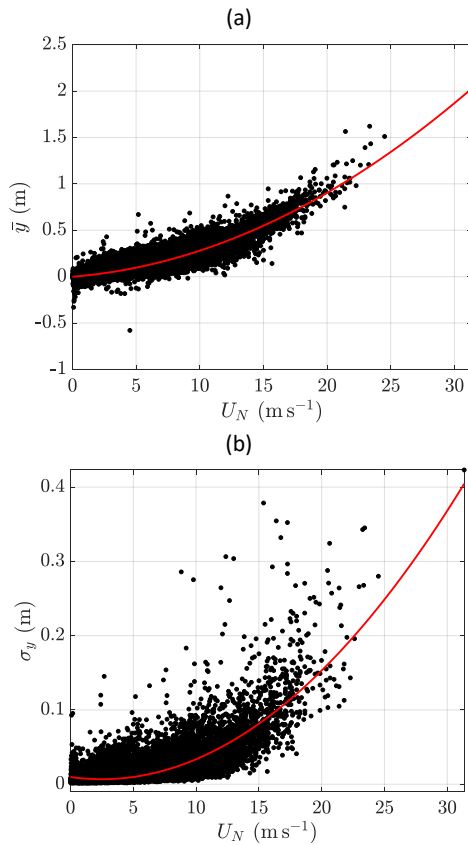


Figure 7. Variability of the 10-minute (a) mean and (b) standard deviation of the lateral response against the normal component of the 10-minute mean wind speed.

### III. ANN-BASED REGRESSION MODEL

#### A. Description of the model

ANNs have been successfully implemented in many fields including pattern recognition, machine learning and civil engineering (Bishop, 1996). In the area of SHM, ANNs are one of the most common methods to study the relationship between the response and natural frequencies of bridges and environmental factors (Ni et al., 2009; Laory et al., 2014). In this work, ANNs are employed to generate a non-linear regression

model to estimate time-dependent lateral and heaving responses with respect to variation of wind, temperature, and traffic. Inputs and outputs of the regression model are 10-minute average statistics and are described in Figure 9. It should be noticed that the time information is used to model traffic data.

Using the Neural Network toolbox of MATLAB, the two-layer feed-forward ANN is implemented and trained by using the monitoring data in 2015 and 2016. The training process aims to iteratively evaluate ANN parameters; this is accomplished if the sum-of-square error  $E = \sum_{i=1}^N [y_i - f_{ANN}(x_i)]^2$  between actual data  $y_i$  and ANN estimates  $f_{ANN}(x_i)$  using input  $x_i$  reaches a minimum value ( $N$  is the number of data points used in the training process). The residual, i.e. the difference between the actual data and ANN estimates is used to assess errors of the regression model, which will be discussed in Section III.B.

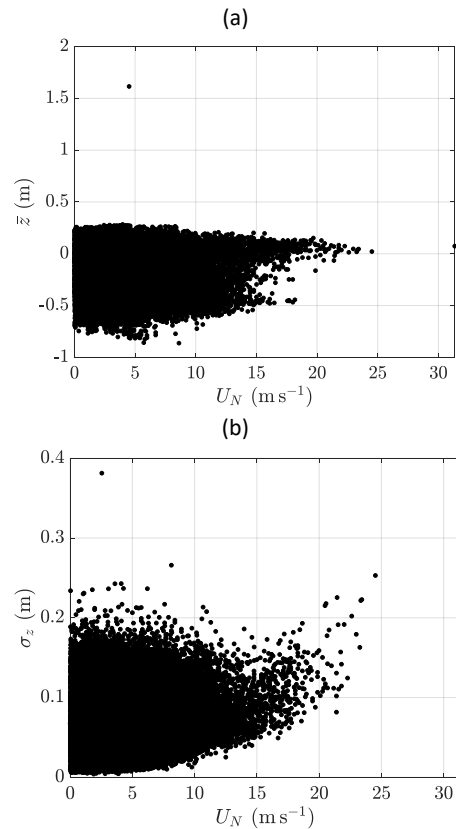


Figure 8. Variability of the 10-minute (a) mean and (b) standard deviation of the heaving response against the normal component of the 10-minute mean wind speed.

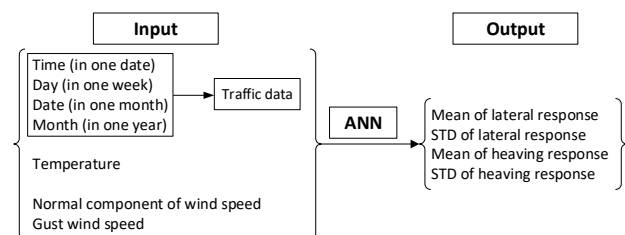


Figure 9. Description of inputs and outputs of ANN-based regression model.

### B. Validation study

Taking a two-week period of normal operation of the FRB (from 01 to 15/08/2016) as an example, Figure 10 and Figure 11 compare estimates obtained from the ANN-based regression model to the actual 10-minute average statistics of the bridge response. In addition, upper and lower bounds are included, which represents the 95% confidence limits of the ANN estimates based on a normal distribution. This approach to quantify errors associated with the ANN estimates was reasonable since residuals between the actual data and ANN estimates were found to closely follow the normal distribution. An example of the residual of the standard deviation of the heaving response  $\sigma_x$  is shown in Figure 12.

In general, the estimates produced by the ANN-based regression model are in a good agreement with the actual data. As shown in Figure 10, the regression model is capable of reproducing the trends and patterns in the lateral response. This includes the event occurring on 07/08/2016 when, under effects of strong wind, the lateral movement of the mid span was larger compared to other days in this period. More importantly, this regression model also successfully models the diurnal patterns observed in the heaving response. Differences between the bridge response on weekdays and at weekends are also captured by the ANN estimates (Figure 11).

It should be noticed that, in Figure 10 and Figure 11, most of the actual data points lie within the 95% confidence limits of the ANN estimates, except to 07/08/2016 when the model underestimates the wind-induced lateral response. Nevertheless, together with an ability to reproduce the trends and diurnal patterns in the bridge response, this error behaviour shows the validity of the ANN-based regression model and that it can be used for further studies.

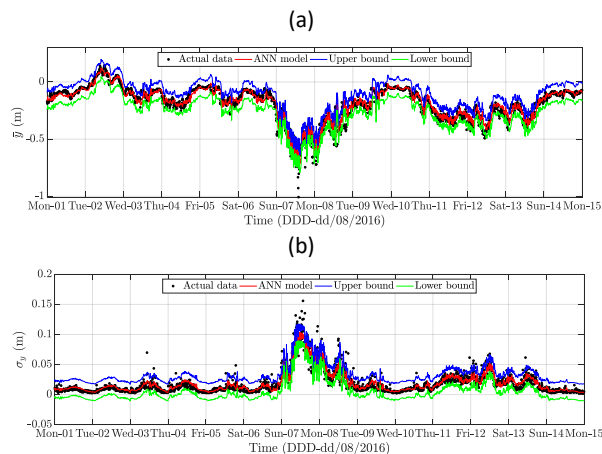


Figure 10. Results of the ANN-based regression models on estimating the 10-minute (a) mean and (b) standard deviation of the lateral response (from 01 to 15/08/2016).

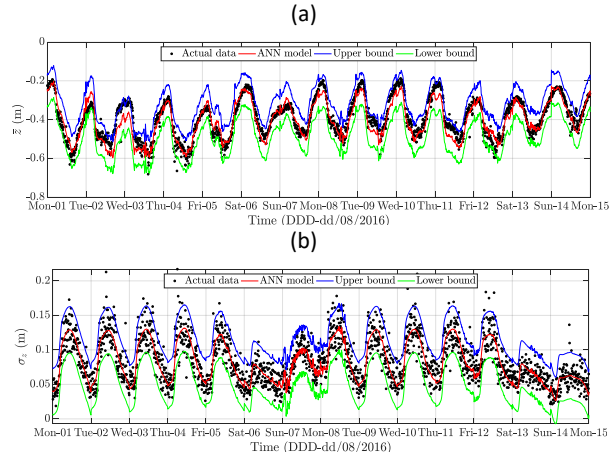


Figure 11. Results of the ANN-based regression model on estimating the 10-minute (a) mean and (b) standard deviation of the heaving response (from 01 to 15/08/2016).

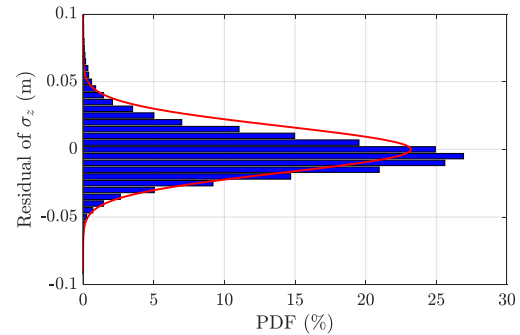


Figure 12. An example of the probability distribution of ANN residuals.

### C. Application of the model

In this section, the usability of the ANN-based regression model generated in Section III.B is investigated in terms of separating traffic-induced effects from the bridge response. The 10-minute mean of the lateral response and the 10-minute standard deviation of the heaving response are considered in this study.

Figure 13 shows a comparison between the actual wind-induced response and the one estimated from the regression model under the influence of wind, temperature and traffic. It is evident that the regression model is capable of modelling the dependence of the mean lateral response on the normal component of the mean wind speed (Figure 13a). On the other hand, as shown in Figure 13b, the regression model underestimates the heaving response. This issue may be due to the fact that the time information is used to reproduce traffic data, which leads to a lower estimation of traffic on some days. More importantly, as observed in the actual data, the outcome of the ANN model shows no clear wind-induced effects on the standard deviation of the heaving responses, which is caused by the dominant influence of traffic.

By adjusting the time information in the input of the regression model, the traffic-induced effects on the

bridge response can be minimised. In Figure 14 *Error! Reference source not found.*, the ANN estimates having traffic-induced effects being minimised are plotted in a comparison with the actual data. It is evident that no significant variations on the relationship between the mean lateral response and the normal component of the mean wind speed are observed (Figure 14a). This indicates that traffic poses very minimal effects on the lateral movement of the bridge as discussed in Section 2.3. On the other hand, dramatic changes are evident on the plot of the standard deviation of the heaving response (Figure 14b). By alleviating traffic-induced effects, a clear quadratic relationship is revealed, particularly at wind speeds higher than 5  $\text{m s}^{-1}$ , which was not observed in Figure 13b. At lower wind speeds, the spread of ANN estimates significantly reduced from 0.15m to 0.05m approximately. These results not only indicate the strong influence of traffic on the heaving response but also demonstrate the great potential of this ANN-based regression model in decoupling effects due to wind, temperature and traffic.

#### IV. CONCLUSION

In this paper, the current progress of the GeoSHM Demonstration Project has been discussed focusing on understanding and modelling some aspects of the baseline performance of the FRB. Using the monitoring data in 2015 and 2016, the ANN-based regression model has been generated to model the dependence of the lateral and heaving responses on wind, temperature and traffic. Residuals between the actual data and the ANN-estimates have been utilised as a means to assess effectiveness of the regression model. Since residuals were found to follow normal distributions, 95% confidence intervals were evaluated to define the upper and lower bounds of ANN estimates. By implementing this regression model, trends and diurnal patterns in the bridge responses were successfully captured. More importantly, the selected results showed that, by varying corresponding inputs, this ANN-based regression model offered a means to separate effects of wind from those of temperature and traffic.

#### V. ACKNOWLEDGEMENTS

The authors would like express their gratitude to the European Space Agency for sponsoring the GeoSHM Demonstration Project. In addition, Amey PLC., Transport Scotland, and China Railway Major Bridge Reconnaissance and Design Institute Co., Ltd. are all acknowledged for their supports and provision of resources.

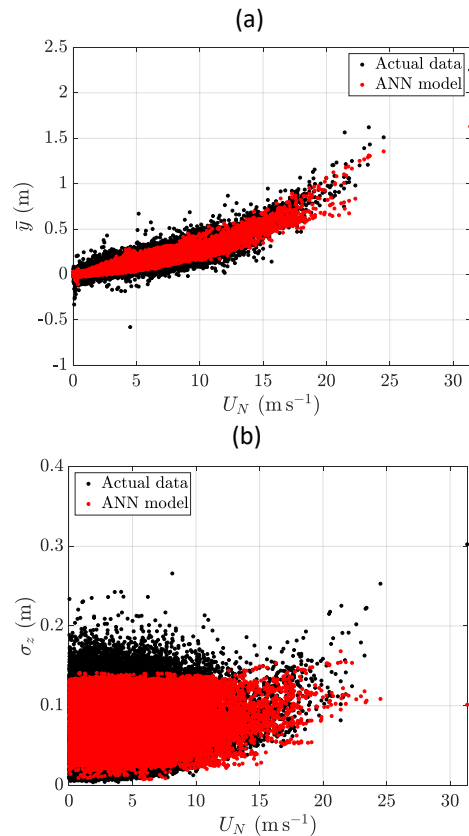


Figure 13. Results of the ANN-based regression model on estimating wind-induced responses under in the influence of wind, traffic and temperature.

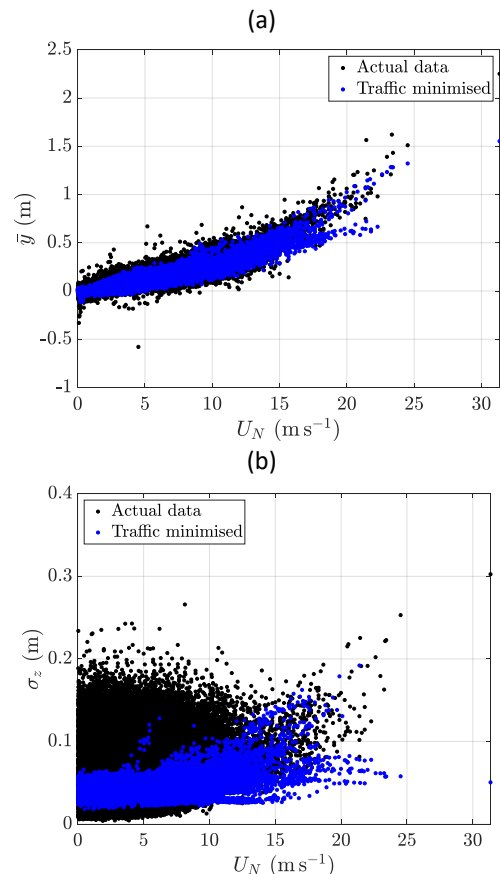


Figure 14. Results of the ANN-based regression model on estimating wind-induced responses when traffic-induced effects are minimised.

### References

- Bishop, C. (1996). *Neural Networks for pattern recognition*. USA: Oxford University Press.
- Chen, Q., W. Jiang, X. Meng, P. Jiang, K. Wang, Y. Xie, J. Ye (2018). Vertical deformation monitoring of suspension bridge tower using GNSS: A case study of the Forth Road Bridge in UK. *Remote Sensings*, Vol 10, No. 364.
- Cross, E.J., K.Y. Koo, J.M.W. Brownjohn, K. Worden. (2013). Long-term monitoring and data analysis of the Tamar Bridge. *Mechanical Systems and Signal Processings*, Vol 35, No. 1, pp 16-34.
- Dervilis, N., K. Worden, E.J. Cross (2015). On robust regression analysis as a means of exploring environmental and operational conditions of SHM data. *Journal of Sound and Vibration*. Vol 327, pp 279-296.
- ESA Website: GeoSHM Demo Projecta-GNSS and EO for Structural Health Monitoring of Bridges – Demonstration. Available at: <https://business.esa.int/projects/geoshm-demo-project> (accessed on 28 March 2018).
- Failure Knowledge Database. Available online: [www.shippai.org/fkd/en/cfen/CD1000144.html](http://www.shippai.org/fkd/en/cfen/CD1000144.html) (accessed on 25 March 2019).
- Laory, I., T.N. Trinh, I.F.C Smith, J.M.W. Brownjohn (2014). Methodologies for predicting natural frequency variation of a suspension bridges. *Engineering Structures*, Vol. 80, pp 211-221.
- Liao, M., T.A. Okazaki (2009). Computational study of the I-35W bridge collapse (CTS09-29). Centre for Transportation Studies, University of Minnesota, Minneapolis, USA, 2009.
- Meng, X., D.T. Nguyen, Y. Xie, J.S. Owen, P. Psimoulis, S. Ince, Q. Chen, J. Ye, P. Batia (2018). Design and implementation of a new system for large bridge monitoring – GeoSHM. *Sensors*, Vol 18, No. 775.
- Meng, X., Y. Xie, P. Psimoulis, D.T. Nguyen, J.S. Owen, G. Ye, L. Wu, S. Pan, J. Qian, P. Bhatia, B. Valentine, P. Madden (2018). Design and implementation of the new system for long-span bridge monitoring – from GeoSHM to iSHM. In: *Proc. Of the 4<sup>th</sup> Joint International Symposium on Deformation Monitoring (JISDM2019), Athens, Greece*.
- Miami Herald. Available online: [www.miamiherald.com/news/local/community/miami-dade/west-miami-dade/article207358659.html](http://www.miamiherald.com/news/local/community/miami-dade/west-miami-dade/article207358659.html) (accessed on 23 March 2019).
- Ni, Y.Q., H.F. Zhou, J.M. Ko (2009). Generalization capability of neural network models for temperature-frequency correlation using monitoring data. *Journal of Structural Engineering*, Vol 135, No. 10, pp 1290-1300.
- The Guardian. Available online: [www.theguardian.com/cities/2019/feb/26/what-caused-the-genoa-morandi-bridge-collapse-and-the-end-of-an-italian-national-myth](http://www.theguardian.com/cities/2019/feb/26/what-caused-the-genoa-morandi-bridge-collapse-and-the-end-of-an-italian-national-myth).